Influence of amorphous structure on polymorphism in vanadia

Kevin H. Stone,[1,a,b] Laura T. Schelhas,[1,a] Lauren M. Garten,[2] Badri Shyam,[1,c] Apurva Mehta,[1] Paul F. Ndione,[2] David S. Ginley,[2] and Michael F. Toney[1]
[1]*Stanford Synchrotron Radiation Lightsource, SLAC National Accelerator Laboratory, Menlo Park, California 94025, USA*
[2]*National Renewable Energy Laboratory, Golden, Colorado 80401, USA*

(Received 26 April 2016; accepted 29 June 2016; published online 13 July 2016)

Normally we think of the glassy state as a single phase and therefore crystallization from chemically identical amorphous precursors should be identical. Here we show that the local structure of an amorphous precursor is distinct depending on the initial deposition conditions, resulting in significant differences in the final state material. Using grazing incidence total x-ray scattering, we have determined the local structure in amorphous thin films of vanadium oxide grown under different conditions using pulsed laser deposition (PLD). Here we show that the subsequent crystallization of films deposited using different initial PLD conditions result in the formation of different polymorphs of VO_2. This suggests the possibility of controlling the formation of metastable polymorphs by tuning the initial amorphous structure to different formation pathways. [http://dx.doi.org/10.1063/1.4958674]

Many technologically relevant materials are in fact kinetically stabilized and not at their true thermodynamic free energy minimum, i.e., they are metastable. These kinetically stabilized materials can show improved functionality over their thermodynamically stable counterparts. One specific example of such metastability is the phenomena of polymorphism, where the same chemical composition exhibits different crystal structures. For a particular set of conditions, there can be only one thermodynamically favorable ground state; any other polymorphs which exist under those conditions are necessarily metastable. One remarkable example of this is the vanadium oxide family of materials which, in addition to a large number of oxides, may be found in many polymorphic forms for a given stoichiometry. Vanadium dioxide itself can be found in at least eight different polymorphs which appear to have been stabilized at ambient conditions without the addition of other stabilizing elements.[1–8]

Historically there are a number of approaches to targeting a particular polymorph. One is to adjust conditions so that the desired phase becomes the lowest energy one, either through control of strain, pressure, or temperature, which then may be frozen in by quenching or carefully returning to standard conditions. A second is to introduce an additional energetic consideration, such as strain and interfacial energy for epitaxial films or surface energy for small crystallites, where the energy of the bulk structure no longer dominates. A third is to kinetically trap a phase other than the thermodynamically favored one by careful control over reaction kinetics. In the case of this third approach, it becomes possible to stabilize amorphous structures, which may be considered a metastable phase as amorphous structures are in general higher in energy than the corresponding ordered structure.[9] However, there has never been a concerted approach to understand how to form an amorphous precursor to get a particular polymorph upon annealing. If this could be accomplished, it would provide a powerful approach for targeting a given polymorph.

---

[a]K. H. Stone and L. T. Schelhas contributed equally to this work.
[b]Author to whom correspondence should be addressed. Electronic mail: khstone@slac.stanford.edu
[c]Current address: Department of Chemistry, Washington College, Chestertown, Maryland 21620, USA.

While metastable polymorphs promise exciting materials properties, it is difficult to predict their formation pathways. A number of approaches have been explored in the literature in an attempt to control the crystallization of VO_2.[10,11] One method of growing materials far from equilibrium is pulsed laser deposition (PLD). PLD provides a number of tunable experimental parameters which may affect the formation of different vanadia polymorphs. As PLD inherently yields thin films, there is an opportunity to epitaxially stabilize different polymorphs, wherein the strain energy caused by lattice matching the film to the substrate may effectively change the ground state polymorph. Indeed, this has been successfully used to tune the metal-insulator transition temperature from the M1- to the R-phase of VO_2, evidently changing the effective ground state phase for different temperatures.[12] Careful choice of the substrate surface can also help direct polymorph formation by minimizing the interfacial energy between the substrate and a particular polymorphic form of the film.[13,14] Lattice matching and strain considerations are only a part of this approach where the chemical environment of each atom and the associated energetics must be considered as well. Apart from epitaxial stabilization, by varying the target and oxygen partial pressure, pO_2, during deposition, the chemistry can effectively be controlled, although in the case of vanadia this must be done carefully to avoid moving off stoichiometry for VO_2. Importantly, PLD offers the ability to control the crystallization kinetics of film formation. By tuning of the substrate temperature and the laser repetition rate and energy, one can affect the kinetics of deposition and control film formation and crystallization. This has been demonstrated for polymorphic control of VO_2 on $SrTiO_3$ substrates.[11]

Within amorphous materials, it is possible to have a wide range of local structures, and even on a bulk level glasses with identical composition can have varying properties due to their local structure.[15] In oxides, this is thought to be due to the natural formation of cation-oxide polyhedra, which may then interconnect in various ways with widely varying relative orientations to form random network structures.[16] While such structural differences are difficult to describe owing to the nature of the amorphous structure, they may have profound consequences for a material behavior. In addition, if glassy materials are subsequently crystallized, the potential influence of this local structure on the formation of long range order is widely unexplored. However, one may consider the likely possibility that local ordering may act as a seed to favor the formation of a given crystal structure, much like the concept of melt memory in the polymorphism of organic small molecules.[17]

Using pulsed laser deposition onto room temperature glass substrates, we have observed the growth of amorphous vanadia thin films. Following the work of Srivastava *et al.*,[11] we chose to use pulsed laser deposition to grow amorphous vanadia films using different laser repetition rates. Using a recently developed grazing incidence approach to total scattering, we were able to determine the local structure of these amorphous films through pair distribution functions, an approach we term Grazing Incidence Pair Distribution Function (GIPDF).[18] In this approach it is possible to carefully control the penetration depth into the film and substrate through control of the incidence angle.[19] We observed that amorphous films have mid-range order up to roughly 1 nm which can be varied by the film growth conditions. The films were then annealed and diffraction collected *in situ* to determine the formation of any crystalline phases. We find that the starting amorphous phase influences the final crystalline form of the film, representing a possible new mechanism for stabilizing different polymorphs.

Thin films of nominal composition VO_2 were grown via PLD on Corning's Eagle XG glass substrates. A KrF excimer laser (Spectra-Physics) operating at 248 nm with a pulse duration of 20 ns was used. The beam was focused on a commercial 1 in. target of V_6O_{13} with a laser fluence of 2 J/cm^2 on the target surface. The pO_2 was maintained at 10^{-4} Torr with deposition onto a room temperature substrate yielding films of nominal thickness of 200 nm. Films were deposited at pulse repetition rates of 2, and 10 Hz with all other parameters held fixed. Films were smooth (~0.8 nm rms roughness) and continuous over an area of 5×5 cm.

GIPDF measurements were made at SSRL beamline 10-2. X-rays of energy 22.5 keV were incident on the sample at an angle of 0.1°, above the critical angle for total reflection of 0.095° but with sufficiently low penetration depth as to not scatter from the glass substrate. This approach allows for scattering to be measured from just the thin film, with sufficiently large illuminated area to give good signal to noise. Scattered x-rays were resolved using Soller slits and detected with a Si vortex detector. Corrections to the scattered intensity were made for the illuminated

volume, Lorentz, and calculated Compton scattering subtracted. Scattered intensity was measured to a maximum Q of 22 $Å^{-1}$ using a variable count time to ensure better counting statistics at higher Q. Corrected intensities were analyzed using the program PDFgetX3.[20]

Films were thermally crystallized by annealing in N_2 at 450 °C with an initial ramp rate of 10°/min. Formation of crystalline phases was monitored *in situ* using a Mar345 image plate on SSRL beamline 11-3 with an x-ray energy of 12.7 keV. Area diffraction images were collected in grazing incidence geometry with an incidence angle of 2° every 2.5 min with 30 s exposure times. Images were calibrated using a LaB_6 standard and integrated using GSAS-II.[21] After annealing, diffraction was collected with a 60 s exposure time. Integrated powder diffraction data was analyzed with TOPAS-Academic.[22]

To determine the effect the laser repetition rate has on the local ordering in our films, we employ GIPDF analysis. Since the films as initially deposited are amorphous, conventional XRD is not possible to determine the ordering of these films. The plots in Figure 1 show the results from the GIPDF experiments on the thin films. Since the films were deposited with the same conditions aside from the laser repetition rate, samples are labelled as 2 Hz and 10 Hz. The local structure of these two films are different as evidenced by the lowest Q correlation feature at approximately 2 $Å^{-1}$ as seen in Figure 1(a) and more clearly in the difference in the real space pair distribution function in Figure 1(b). In Figure 1(b) the main V–O correlations are seen between 1.5 and 2.3 Å and the V–V and various O–O bonds form the peaks between 2.3 and 4 Å. The many small features are termination ripples caused by Fourier transforming the limited data range. The key observation is that there are differences in the local order (atomic pair correlations to a distance of ~1 nm) of two films deposited with different laser repetition rates. However, correlation between the amorphous structure observed and the different VO_x crystalline polymorphs is challenging and beyond the scope of this work.

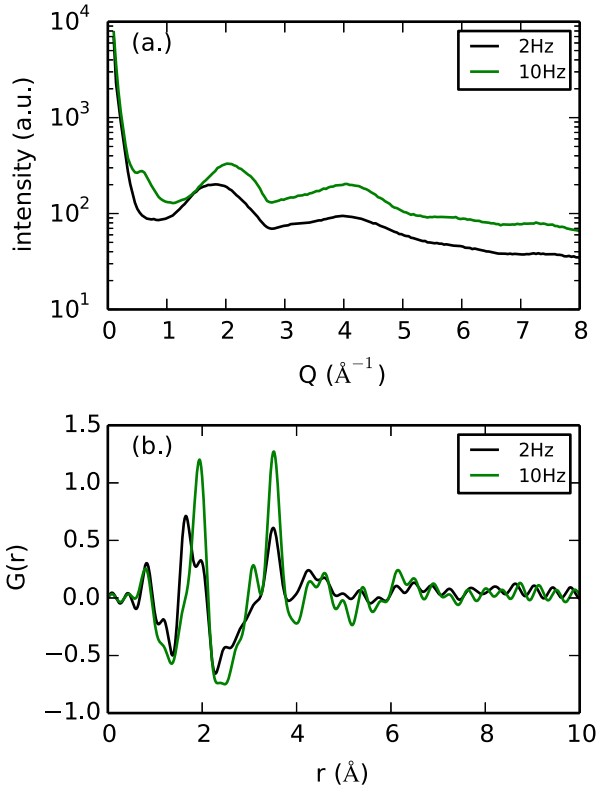

FIG. 1. Total scattering data (a) for the 2 Hz and 10 Hz samples as deposited. The calculated pair distribution function is shown in (b). Total scattering data were collected to a maximum Q of 22 $Å^{-1}$, only the low Q range is shown here, the rapid oscillations seen in (b) are termination ripples due to Fourier transforming a limited data range.

In order to determine if these differences were the result of differences in oxygen stoichiometry, the vanadium K-edge absorption was measured.[23] Both the 2 Hz and 10 Hz films match most closely to V^{4+} and with very similar features, so significant differences in the stoichiometry of the films can be ruled out. However it is worth noting that subtle differences exist in the vanadium x-ray absorption spectra, which could correspond to very small fluctuations in oxygen concentration in addition to variations in the local vanadium environment. For this reason small stoichiometric differences may contribute to the differences seen in the local ordering from GIPDF analysis.

In situ XRD measured during crystallization shows the evolution of the films from the initial amorphous state to the final crystalline polymorphs. Figure 2(a) shows select *in situ* XRD data during crystallization of the 2 Hz film. The plot shows a limited Q range for easier visualization of the phase formation, and example of the full data range and refinement fits for both the 2 Hz and 10 Hz samples can be found in the supplementary material.[23] As the film begins to crystallize, both the expected VO_2 ground state R-phase and a metastable B-phase are present in the film. Over time the intensity of the peaks that correspond to the R-phase develops at partial expense of the B-phase component. This suggests that the crystallization of the B-phase is rapid and the B-phase grains are not able to grow under these annealing conditions, whereas the R-phase crystallization is gradual and continues over time before finally leveling out after about an hour and a half of annealing. Figure 2(b) plots the phase fraction of the B- and R-phases as a function of time. Here we can clearly see that the film is predominately in the metastable B-phase (~60%). The R-phase of the film transitions to the M1-phase at room temperature with the phase transition distinguished by the dashed line of the plot.

In marked contrast, Fig. 3 shows that for the 10 Hz sample, only the VO_2 R-phase is seen in the film. In Figure 3(b), we can see that the formation of the R-phase is quite rapid, with no increase in

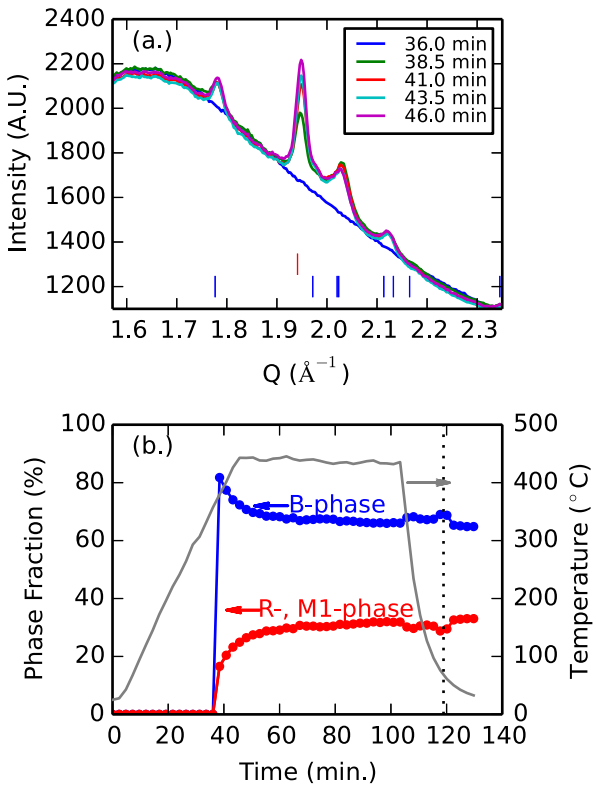

FIG. 2. Evolution of crystalline phases during annealing for the 2 Hz sample. Selected region of the scattering is shown in (a) illustrating the growth of both the R- and B-phases at different time points into the anneal. The relative phase fraction for the two phases is shown in (b) along with the temperature profile for the annealing process. After initial formation of the B-phase the R-phase develops at partial expense of the B-phase component.

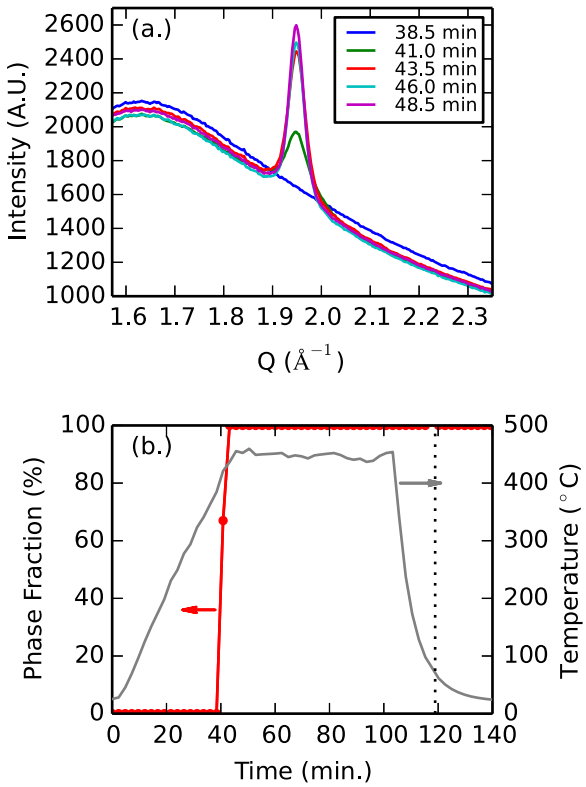

FIG. 3. Evolution of crystalline phases during annealing for the 10 Hz sample. Selected region of the scattering is shown in (a) illustrating the growth of both the R-phase with no evidence of the B-phase at different time points into the anneal. The scale factor for the R-phase used in the refinement is shown in (b) along with the temperature profile for the annealing process. Evidently the R-phase develops rapidly with no increase in crystallinity with prolonged annealing.

crystallinity after the initial point signaling the onset of crystallization. Again the R-phase makes the expected transition to the M1-phase near room temperature (dashed line).

Comparison of the *in situ* XRD data presented in Figures 2 and 3 clearly shows a large difference in the final film structure when comparing the 2 Hz and 10 Hz films. This shows that the differences seen in the as deposited amorphous precursor films influence the final crystalline film formation. Even though we cannot determine if subtle differences in oxygen stoichiometry of the initial amorphous films are the reason for the variations in local structure, the final films have crystallized into VO_2 and show no evidence for V_2O_5 or any sub-oxides. Calculated pair distribution functions of the observed polymorphs, the B-, R-, and M1-phases, show similar V–O and V–V bond lengths to those observed in the amorphous films; however, no obvious correlation exists between the amorphous structure and the polymorphs into which it crystallizes, suggesting that the amorphous films are not simply nanocrystalline phases of the end member polymorphs but rather have distinct local structures.

The formation of the B-phase in the 2 Hz sample can be seen to form preferentially at early time points, consistent with Ostwald's rule that states the less stable polymorph will crystallize first.[24,25] More specifically, the state which will be sought will be the one nearest in stability to the original state, implying the possibility of polymorph control through the amorphous state. While the local structure of the 2 Hz film prior to crystallization is not obviously more closely related to the B-phase then either the R- or M1-phases, it is possible that this represents the lower energy amorphous phase which is stabilized by the slower deposition rate. Although inconsistent with a locally seeded B-phase structure, evidently the transformation pathway from this amorphous starting point more easily leads to the metastable polymorph than to the thermodynamically preferred crystalline R-phase ground state. Interestingly, the more rapidly deposited film, which one

would assume to be higher in energy, transforms directly to the crystalline ground state with little to no change upon further annealing; this is in contrast to the slower transformation observed in the 2 Hz sample. Evidently, the reaction kinetics associated with crystallization from an amorphous film will depend on the free energy of the amorphous structure. Further work is needed to understand the relationship between the structure of the amorphous phase and the preferred crystalline polymorph; however the relationship is evidently not as simple as both having similar local structures which, in the amorphous phase, may act as seeds for crystalline growth. We propose that control over local order through thin film deposition conditions may provide distinct starting points for subsequent crystallization, potentially representing an unexplored route to the stabilization of metastable polymorphs.

The authors would like to thank Ronald Marks for assistance with SSRL beamline 10-2 where the GIPDF measurements were performed and Tim Dunn for assistance with SSRL beamline 11-3 where the *in situ* x-ray diffraction during crystallization was measured. We would also like to thank Matthew Latimer and Erik Nelson for assistance with SSRL beamlines 4-1 and 4-3 where the XAS data were collected. This work was supported as part of the Center for Next Generation Materials by Design (CMGMD), an Energy Frontier Research Center funded by the U.S. Department of Energy, Office of Science, Basic Energy Sciences under Contract No. DE-AC36-08GO28308. Use of the Stanford Synchrotron Radiation Lightsource, SLAC National Accelerator Laboratory, was supported by the U.S. Department of Energy, Office of Basic Energy Sciences under Contract No. DE-AC02-76SF00515.

[1] G. Andersson, C. Parck, U. Ulfvarson, E. Stenhagen, and B. Thorell, Acta Chem. Scand. **10**, 623 (1956).
[2] R. Heckingbottom and J. W. Linnett, Nature **194**, 678 (1962).
[3] Y. Oka, T. Yao, and N. Yamamoto, J. Solid State Chem. **86**, 116 (1990).
[4] F. Théobald, R. Cabala, and J. Bernard, J. Solid State Chem. **17**, 431 (1976).
[5] D. Hagrman, J. Zubieta, C. J. Warren, L. M. Meyer, M. M. J. Treacy, and R. C. Haushalter, J. Solid State Chem. **182**, 178 (1998).
[6] L. Liu, F. Cao, T. Yao, Y. Xu, M. Zhou, B. Qu, B. Pan, C. Wu, S. Wei, and Y. Xie, New J. Chem. **36**, 619 (2012).
[7] Y. Wang, Z. Zhang, Y. Zhu, Z. Li, R. Vajtai, L. Ci, and P. M. Ajayan, ACS Nano **2**, 1492 (2008).
[8] H. T. Evans and M. E. Mrose, U.S. Geological Survey, 1954.
[9] D. Turnbull, Contemp. Phys. **10**, 473 (1969).
[10] N. Bahlawane and D. Lenoble, Chem. Vap. Deposition **20**, 299 (2014).
[11] A. Srivastava, H. Rotella, S. Saha, B. Pal, G. Kalon, S. Mathew, M. Motapothula, M. Dykas, P. Yang, E. Okunishi, D. D. Sarma, and T. Venkatesan, APL Mater. **3**, 026101 (2015).
[12] F. C. Case, J. Vac. Sci. Technol., A **2**, 1509 (1984).
[13] A. Zur and T. C. McGill, J. Appl. Phys. **55**, 378 (1984).
[14] H. Ding, S. S. Dwaraknath, L. Garten, D. Ginley, and K. A. Persson, ACS Appl. Mater. Interfaces **8**, 13086 (2016).
[15] H. W. Sheng, H. Z. Liu, Y. Q. Cheng, J. Wen, P. L. Lee, W. K. Luo, S. D. Shastri, and E. Ma, Nat. Mater. **6**, 192 (2007).
[16] W. H. Zachariasen, J. Am. Chem. Soc. **54**, 3841 (1932).
[17] J. Bernstein, Cryst. Growth Des. **11**, 632 (2011).
[18] B. Shyam, K. H. Stone, R. Bassiri, M. Fejer, M. F. Toney, and A. Mehta, "Measurement and modeling of short and medium range order in amorphous Ta2O5 thin films," Sci. Rep. (submitted).
[19] D. R. Blasini, J. Rivnay, D.-M. Smilgies, J. D. Slinker, S. Flores-Torres, H. D. Abruña, and G. G. Malliaras, J. Mater. Chem. **17**, 1458 (2007).
[20] P. Juhás, T. Davis, C. L. Farrow, and S. J. L. Billinge, J. Appl. Crystallogr. **46**, 560 (2013).
[21] B. H. Toby and R. B. Von Dreele, J. Appl. Crystallogr. **46**, 544 (2013).
[22] A. Coelho, TOPAS-Academic v5 (2012), http://www.topas-academic.net.
[23] See supplementary material at http://dx.doi.org/10.1063/1.4958674 for vanadium K-edge x-ray absorption spectra (Fig. S1) and the Rietveld refined powder diffraction data for the crystallized samples during crystallization (Figs. S2 and S4) as well as after subsequent cooling to room temperature (Figs. S3 and S5).
[24] W. Ostwald, Z. Phys. Chem. **22**, 289 (1897).
[25] T. Threlfall, Org. Process Res. Dev. **7**, 1017 (2003).